American Mineralogist, Volume 70, pages 388–394, 1985

TEM/STEM microanalysis of Holocene fresh-water magnesian carbonate cements from the Coast Range of California

DAVID F. BLAKE[1] AND DONALD R. PEACOR

Department of Geological Sciences
The University of Michigan, Ann Arbor, Michigan 48104

Abstract

Four magnesian carbonate Holocene fresh water cements from the Coast Range of California were investigated using X-ray and electron microbeam techniques. These travertines and conglomerate cements include three dolomite cements, which have compositions from $Ca_{0.59}Mg_{0.41}CO_3$ to $Ca_{0.55}Mg_{0.45}CO_3$. The fourth cement is a magnesian calcite of composition $Ca_{0.77}Mg_{0.23}CO_3$. Both dolomite and magnesian calcite cements exhibit weakened and broadened basal plane reflections in powder XRD patterns.

All cements exhibit a heterogeneous microstructure in bright field TEM micrographs. The cements are mosaics of submicron-sized crystals with partial topotaxial orientation. Aside from mosaic spreading, diffraction maxima in electron diffraction patterns show no diffuseness or streaking. Ordering diffractions are present in electron diffraction patterns of the dolomite cements but are not observed in equivalent patterns from the magnesian calcite cement.

Cation disorder in the dolomites appears to be by substitution of Ca into Mg planes, rather than by a mixed layering mechanism. The calcite-type cement shows greater ranges of composition between individual crystals than do the dolomite-type cements. Dolomite ("protodolomite") compositions are consistent with the existence of a metastable, partially ordered reactive intermediate. STEM microanalytical data demonstrate that broadening and diffuseness in powder XRD maxima are due to microscale compositional heterogeneity rather than structural phenomena.

Introduction

Barnes and O'Neil (1971) describe Holocene magnesian carbonate cements precipitated in perennial streams in the Coast Range of California. These cements result from the mixing of Ca^{2+}–OH^- rich waters with Mg^{2+}–HCO_3^- rich waters flowing from ultramafic and serpentinite terranes. The resulting cements, according to the authors, are primary precipitates which form in C and O isotopic equilibrium and thermodynamic disequilibrium. Two types of magnesian carbonate solid solutions are described on the basis of powder XRD patterns.:

1. Magnesian calcite solid solutions exhibit no ordering reflections, and weakened basal plane reflections in powder XRD patterns.

2. Dolomite solid solutions, ranging from $Ca_{0.6}Mg_{0.4}CO_3$ to $Ca_{0.5}Mg_{0.5}CO_3$, yield the allowed basal plane reflections and weakened ordering reflections such as 01.5 in powder XRD patterns.

The precipitation of magnesian calcites and calcian dolomites ("protodolomites", according to the terminology of Gaines, 1974) in such low salinity waters is unique. Four cements were chosen which represent the range of composition and structure in the samples described by Barnes and O'Neil (1971). "Del Puerto #1", "Bear Creek #2", and "Bear Creek #3" cements are dolomites of average composition $Ca_{0.59}Mg_{0.41}CO_3$ to $Ca_{0.55}Mg_{0.45}CO_3$. The "Bear Creek #1" cement is a magnesian calcite having a composition of $Ca_{0.77}Mg_{0.23}CO_3$.

TEM/STEM microanalysis is a relatively new technique in the geological sciences, and provides for concurrent high resolution structural and chemical analysis of suitably prepared samples. The characterization of structural and chemical heterogeneities present in these cements (as implied from the powder XRD data) will lend insight into primary processes of carbonate precipitation. Furthermore, it is of interest to study cation order-disorder relationships in these cements, which effectively span the solvus gap between calcite and dolomite. Lastly, a comparison of the microstructure and microchemistry of these cements with similar data from cements formed in saline and hypersaline water should provide a better understanding of the influence of high salinity in the precipitation of such metastable phases.

Methods

Samples to be analyzed by XRD, TEM, and STEM microanalysis were prepared as follows: Centimeter-sized pieces of the material were disaggregated in a mortar and pestle, and ground until

[1] Present address: Surface Science Laboratories, 1206 Charleston Rd., Mountain View, CA 94043.

0003–004X/85/0304–0388$02.00

a uniform sand-sized mixture was obtained. Preliminary heavy liquid separation was carried out in bromoform-acetone mixtures using a separatory funnel. The purified "calcite + dolomite" fractions ($2.67 < d < 2.86$) were then ground to a powder. Using the same heavy liquid preparations, the samples were further purified by centrifugation. The resulting "calcite + dolomite" fractions were cleaned in acetone and air dried. In the final fractions, no more than 5–10% impurities (largely quartz) were present.

For X-ray diffraction analyses, powder mounts were scanned from 15 to 55 degrees 2θ, using Cu$K\alpha$ radiation. Mole% $MgCO_3$ was determined from the displacement of the 10.4 diffraction maximum by comparison to lattice parameter vs. composition curves prepared from Goldsmith and Heard (1961).

TEM/STEM samples were prepared as follows: A 50:50 mixture of each sample was made with TORRSEAL™ epoxy resin. This mixture was then pressed between two glass slides coated with silicon mold release. After 24 hours, the slides were removed, and the thin film of epoxy + randomly oriented grains was cleaned in acetone. A 3-mm-diameter support washer was epoxied to the material, and the washer, with its attached disk of material, was cut away from the surrounding bulk. The material was further thinned in an argon ion-mill at 6.0 kV, and 15 degrees milling angle. In the resulting ion-thinned sections, electron-transparent grains, held in place by the epoxy, are present on the perimeter of the central hole. This sample preparation technique is superior to the conventional "crushed grain" mounting technique, since large electron-transparent regions are produced. In addition, unlike conventionally ion-thinned specimens, such "squashed grain" preparations are less susceptible to continuum fluorescence effects (see Allard and Blake, 1982) or other spurious effects caused by X-ray spectral contamination. While TORRSEAL™ epoxy contains a variety of silicate phases used as filler material, the bulk of the epoxy is resin, and continuum fluorescence effects are minimal relative to conventionally prepared self-supported specimens.

Analyses for Mg and Ca were recorded in STEM mode and data were quantified using the Cliff-Lorimer (ratio) technique (Cliff and Lorimer, 1972). Ca$K\alpha$/Mg$K\alpha$ X-ray intensity ratios were compared to a working curve prepared from Ca- and Mg-containing phases of known composition (see Blake and Peacor, 1981 and Blake et al., 1983 for a further description of the analytical technique). Quantitative analyses were performed at 100 kV accelerating voltage and spectra were recorded over 200 second counting times with a beam current of 0.5 nA and a nominal beam diameter of 100Å. Areas chosen for analysis met the "thin film criterion" (Goldstein, 1979) which holds for Mg/Ca data in materials of this type which are 3000Å or less in thickness. Results were analyzed statistically by a technique developed for use with data of this type (Blake et al., 1983). Utilizing the STEM technique it is possible to achieve a lateral spatial resolution approaching 300Å in thin samples. However, carbonates are very susceptible to mass loss (electron beam damage) under these conditions and analyses reported here were recorded by scanning the beam over 1000Å square areas of material.

Results

Powder XRD of cements

Cements purified by heavy liquid separation and centrifugation were analyzed by powder XRD using Cu$K\alpha$ radiation. Peaks in the high 2θ region of diffractometer scans are broad and diffuse, typical of recent natural and synthetic magnesian calcites and dolomites. The 00.6 maximum is weakened but detectable in the dolomite cements, but not observed in the magnesian calcite cement. Figure 1 shows diffractometer traces for the four cements.

Due to the small crystal size of the cements (sub-μm to 1–2 μm in diameter), quantitative microanalysis using electron microprobe was precluded. Powder XRD patterns were therefore used to estimate $MgCO_3$ content of the dolomite and calcite cements. While least-squares refinement of lattice parameters is the most accurate means of determining lattice parameters (and $MgCO_3$ incorporation) from X-ray diffraction patterns, most peaks in the patterns were too broad and diffuse for accurate measurement. The 10.4 peak displacement relative to an internal quartz standard was therefore used to provide an estimate of $MgCO_3$ incorporation, using curves prepared from Goldsmith and Heard (1961). Solid solution of cations such as Mn, Fe, etc. in the calcite structure also causes displacement of diffraction maxima. Qualitative EDS scans using a SEM demonstrated, however that the only major or minor cations present in the cements were Mg and Ca. Compositions are: for dolomite cements, Del Puerto #1, $Ca_{0.59}Mg_{0.41}CO_3$; Bear Creek #2, $Ca_{0.58}Mg_{0.42}CO_3$; Bear Creek #3, $Ca_{0.55}Mg_{0.45}CO_3$; and for the magnesian calcite cement, Bear Creek #1, $Ca_{0.80}Mg_{0.20}CO_3$. These values are considered to be accurate to within $\pm$1–2 mole%.

SEM of cements

Fracture surfaces of dolomite and magnesian calcite cements were observed with the SEM. The magnesian calcite and dolomite cements are composed of sub-μm sized anhedral crystallites which form subspherical masses 5–10 μm in diameter. As in the marine surface crust cements described by Kocurko (1981) and Blake et al. (1982), the polycrystalline masses appear to show the incipient development of crystal forms. It appears therefore, that the crystallites which comprise each polyhedral mass are in loose topotaxial registry, one to another. Figure 2 shows the typical morphology and appearance of the magnesian calcite and dolomite cements.

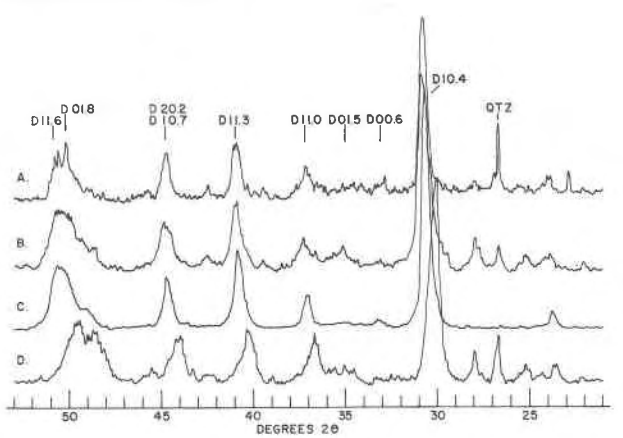

Fig. 1. Powder XRD of dolomite and magnesian calcite cements. (a) Del Puerto #1 dolomite cement ($Ca_{0.59}Mg_{0.41}CO_3$) (b) Bear Creek #2 dolomite cement ($Ca_{0.58}Mg_{0.42}CO_3$) (c) Bear Creek #3 dolomite cement ($Ca_{0.55}Mg_{0.45}CO_3$) (d) Bear Creek #1 magnesian calcite cement ($Ca_{0.80}Mg_{0.20}CO_3$).

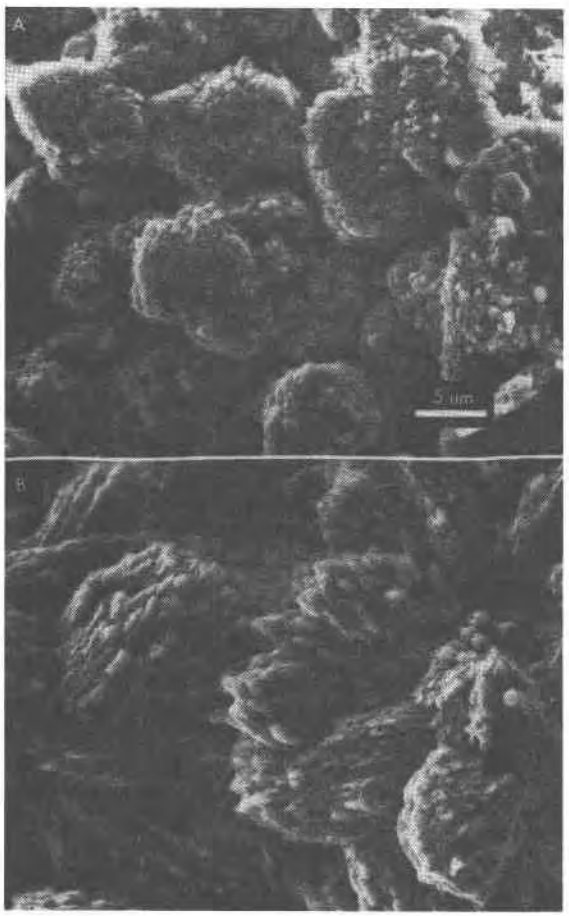

Fig. 2. SEM micrographs of dolomite and calcite cements. (a) Del Pureto #1 dolomite cement. (b) Bear Creek #1 magnesian calcite cement. Magnification is the same in both micrographs.

TEM/STEM microanalysis of cements

Dolomite cements. TEM micrographs of the dolomite cements display a striking "mottled" microstructure when viewed in conventional bright field mode. The microstructure is in contrast in dark field mode for all "*a*" type (non-ordering) reflections. Ordering ("*b*" type) reflections such as 00.3, etc., when used in dark field imaging, produce similar, but less intense contrast features. Figure 3 shows bright and dark field images of the microstructure of the Bear Creek #2 cement, using the 10.4 reflection. Contrast in the images cannot be uniquely explained due to the conditions used for imaging (this is generally true for dark-field imaging). However, this mottled contrast cannot be ascribed to cation order–disorder phenomena, since identical contrast features are seen in the magnesian calcite cement which shows no ordering reflections.

All dolomite grains imaged possess the heterogeneous microstructure, as welll as ordering diffractions such as 10.1, 02.1, and 00.*l*, $l = 2n + 1$. It should be noted that in order to assess the presence or absence of dolomite ordering reflections, diffraction conditions must be carefully controlled. This is because double diffraction, which is a rare event in X-ray diffraction, is very common in electron diffraction. For example, to unambiguously determine the presence of 00.3, the sample must be oriented so that only the 00.*l* systematic row of diffraction maxima is excited. In general, no non-ordering type diffractions should be present in the pattern which can be added vectorially to produce the ordering maximum.

Even using the smallest selected area diffraction aperture, which limits the area contributing to the electron diffraction pattern to slightly less than 1.0 μm laterally, mosaic structure (as evidenced by multiple diffraction maxima) is observed. However, the mosaic domains are very nearly in crystallographic (and topotactic) registry, as evidenced by electron diffraction patterns recorded from areas which include a large number of domains. Despite the fine-grained nature of these cements, therefore, crystal nucleation appears to have been via a heterogeneous mechanism. In selected area electron diffraction patterns, the ordering diffractions are discrete points, and show no dif-

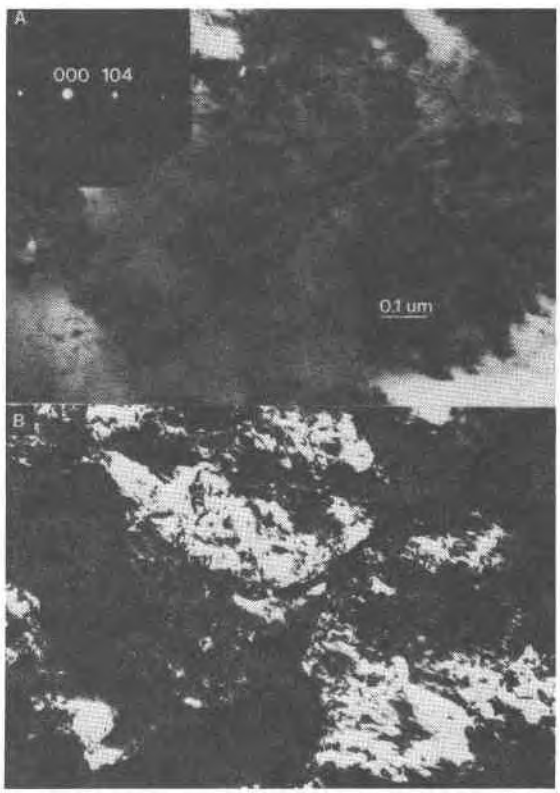

Fig. 3. TEM micrograph of Bear Creek #2 dolomite cement. (a) Bright field micrograph, showing mottled microstructure which is typical of all cements examined under highly diffracting conditions. The contrast is seen to "roll" across the field of view when the crystal is tilted slightly. (b) Dark field TEM micrograph, using 10.4. The mottled microstructure is in strong contrast for all *hk.l* used in bright or dark field imaging. The microstructure highlights irregular mosaic domains, sub-μm in size, which are slightly misaligned, one to another.

Table 1. Summary of STEM microanalytical data from Bear Creek #2 dolomite cement

Crystal #	# Obs.	$MgCO_3$ %	Std. Dev. %	F-Test Results	Comments
1	25	41	3.2	3.2 (24,48)	2,3
2	25	42	4.2	5.4 (24,48)	1,2,3
3	25	46	4.4	7.4 (24,48)	1,2,3
4	10	44	2.6	2.2 (9,48)	2
5	6	31	3.3	2.7 (5,48)	2
6	7	44	1.8	1.1 (6,48)	2
7	15	43	4.7	7.6 (14,48)	1,3
8	8	32	5.1	3.3 (7,48)	2,3
Totals	121	42	5.0	8.7 (120,48)	1,2,3

1. Some anomalous values present which increase the standard deviation, but which could not be removed from the data on an a priori basis.
2. Ordering diffractions identified by electron diffraction.
3. F-test results significant at the 5% level, indicating that Mg incorporation into the structure is homogeneous.

Table 2. Summary of STEM microanalytical data from Del Pureto #1 dolomite cement

Crystal #	# Obs.	$MgCO_3$ %	Std. Dev.	F-Test Results	Comments
1	26	37	4.3	5.3 (25,48)	1,2,3
2	10	34	3.7	3.7 (9,48)	1,2,3
3	25	41	3.4	3.7 (24,48)	1,2,3
4	25	38	2.2	1.3 (24,48)	2
5	10	43	2.4	1.9 (9,48)	2
6	26	39	3.0	2.7 (25,48)	2,3
7	24	38	1.4	0.5 (23,48)	
Totals	146	39	3.7	4.1 (145,48)	1,2,3

1. Some anomalous values present which increase the standard deviation, but which could not be removed from the data on an a priori basis.
2. Ordering diffractions identified by electron diffraction.
3. F-test results significant at the 5% level, indicating that Mg incorporation into the structure is homogeneous.

fuseness or "smearing out" along **c**. This suggests that micro-domains of differing Ca-Mg order along the **c**-axis are not present.

STEM microanalytical data for the Bear Creek #2 dolomite cement are presented in Table 1. The overall average for 121 200-second analyses of individual 0.1 μm areas is $Ca_{0.58}Mg_{0.42}CO_3$. No other cations such as Mn, Fe, etc. were observed in STEM EDS spectra. Sensitivity for detection of these elements under the conditions used for analysis is estimated to be 0.25–0.50 mole%. While individual crystallites are relatively homogeneous, some crystallites (such as crystals 5 and 8 of Table 1) have strikingly lower Mg contents than the average. Crystallites 7 and 8 were part of a single micron-sized grain (and in close topotaxial orientation), and so these compositions do not appear to represent two different cement generations present in the material. It is also of interest that crystallite 8 (31.76 mole% $MgCO_3$) exhibits weak 00.*l* ordering diffractions. This is the lowest Mg content of any dolomite-like material we have examined. STEM microanalytical data for the Del Puerto #1 and Bear Creek #3 dolomite cements are presented in Tables 2 and 3. Results are, within measurement error, not significantly different from the Bear Creek #2 data.

Magnesian calcite cement. TEM micrographs of Bear Creek #1 magnesian calcite cement show the same mottled microstructure as the dolomite cements. The mottling is in contrast for all highly diffracting conditions in bright field mode, and, under dark field imaging conditions, for all "*a*" type diffractions. There is in addition, a mosaic domain structure similar in size and appearance to that found in the dolomite cements.

When properly oriented (highly excited 00.*l*, with *hk.l* out of the diffraction condition to eliminate double-diffraction effects), the dolomite cements exhibit ordering diffractions while the Bear Creek #1 magnesian calcite cement does not. Therefore, the Bear Creek #1 cement is, *sensu stricta*, a magnesian calcite.

The 00.6 reflection, which is not observed in powder XRD patterns, is present in electron diffraction patterns of properly oriented crystals of the magnesian calcite cement. The presence of 00.6 in electron diffraction patterns, and its absence in powder XRD patterns could be due to one or a number of the following: (1) Heterogeneous incorporation

Table 3. Summary of STEM microanalytical data from Bear Creek #3 dolomite cement

Crystal #	# Obs.	$MgCO_3$ %	Std. Dev.	F-Test Results	Comments
1	26	41	2.5	1.8 (25,48)	
2	25	45	2.7	2.6 (24,48)	2
3	15	38	2.0	1.1 (14,48)	
4	25	40	2.7	2.1 (24,48)	1,2
5	20	42	2.6	2.2 (19,48)	2
Totals	111	42	3.4	2.5 (110, 48)	1,2

1. Some anomalous values present which increase the standard deviation, but which could not be removed from the data on an a priori basis.
2. Ordering diffractions identified by electron diffraction.

of Mg could cause a broadening of 00.*l* maxima, which, even in stoichiometric calcite and dolomite samples, are weak in powder XRD patterns (for example, 00.6 has an intensity of 3 in calcite, and 6 in dolomite, relative to 10.4, which is assigned an intensity of 100). (2) Crystallite size has some influence on the nature of powder XRD maxima. Sub-μm sized crystallites would produce a weakening and broadening of diffractions in powder XRD patterns. (3) Depending on the nature of the imperfections present in the structure, or the presence of antiphase domains (for example, CO_3 group disorder of the type discussed by Gunderson and Wenk (1981) and Reeder and Nakajima (1982)), powder XRD diffractions may appear weakened or broadened.

Schneider (1976) listed structure factor calculations for various *hk.l* planes in dolomite. A weakening of diffracted intensities from those planes with a large contribution of C and O would be permissive evidence for disorder in CO_3 groups. However, qualitative analysis of magnesian calcite XRD maxima suggests that CO_3 group disorder does not contribute substantially to the weakening and broadening of 00.*l* diffractions.

We suggest that Mg heterogeneity between and within individual crystallites is the primary cause of peak broadening in the powder XRD patterns. While individual crystallites show relatively discrete diffraction maxima via TEM, *d*-values calculated from electron diffraction patterns are relatively insensitive to compositional fluctuation. For example, if a micron-sized crystal contained volumes of $Ca_{0.5}Mg_{0.5}$ and $Ca_{0.6}Mg_{0.4}$, the difference in the *d*-value for 00.6 would be 0.035Å. This would correspond to a difference of only 0.2 mm between calcite and dolomite 00.6 maxima on an electron diffraction pattern taken at a standard camera length of 120 cm. In powder XRD patterns, such a compositional fluctuation would result in a difference in 2θ (Cu$K\alpha$ radiation) of 0.45 degrees, easily recognizable as broadening in a powder pattern.

STEM microanalytical data from both the dolomite and calcite samples show some degree of Mg/Ca heterogeneity within individual crystals and a larger degree of heterogeneity between crystals. (see Tables 1–4). It is therefore concluded that compositional heterogeneity is responsible for the weakening and spreading of 00.*l* type reflections in powder XRD patterns. Furthermore, such spreading and diffuseness would have a greater effect on *hk.l* planes with large *l* component (i.e., basal planes) than on those with large *h* or *k* component. Assuming a linear relation between calcite and dolomite lattice parameters, $a = 4.99 - (3.64 \times 10^{-3})$ (Mg%) and $c = 17.06 - (2.1 \times 10^{-2})$ (Mg%). For calcite vs. dolomite, $\Delta a/a = 0.0361$ and $\Delta c/c = 0.0598$. Therefore, 00.*l* diffractions are nearly twice as sensitive as *h*0.0 or 0*k*.0 diffractions to compositional change. This would explain the broadening of basal plane diffractions relative to other *hk.l* diffractions in XRD patterns of synthetic and natural low-temperature magnesian calcites.

STEM microanalytical data for the Bear Creek #1 magnesian calcite cement are presented in Table 4. The overall average, for 202 200-second analyses of individual 0.1 μm areas is $Ca_{0.79}Mg_{0.21}CO_3$. As can be seen in Table 4, while only slight heterogeneity is seen within individual crystals, there are marked differences in Mg incorporation between crystals. Crystal #7, for example, contains only about 2.0 mole% $MgCO_3$. While this represents nearly the limit of sensitivity for the analytical conditions used (the peak to background ratio for the Mg$K\alpha$ peak is about 1:5), the results are consistent with the presence of a very low magnesian calcite phase. In addition, since this low magnesian calcite crystal exhibited the mottled microstructure, the microstructure is not a function of Mg incorporation, but rather must be related to some aspect of crystal growth.

Table 4. Summary of STEM microanalytical data from Bear Creek #1 magnesian calcite cement

Crystal #	# Obs.	$MgCO_3$ %	Std. Dev.	F-Test Results	Comments
1	25	24	2.8	1.9 (24,48)	1
2	25	27	3.8	2.5 (24,48)	1,2
3	15	22	2.8	2.0 (14,48)	1
4	16	16	1.5	0.5 (15,48)	
5	26	24	3.3	2.7 (25,48)	2
6	30	25	4.7	5.6 (29,48)	1,2
7	25	2	0.9	1.0 (24,48)	
8	20	26	2.8	1.9 (19,48)	
9	20	15	2.4	1.6 (19,48)	
Totals	202	22	6.8	12.3 (201,48)	1,2

1. Some anomalous values present which increase the standard deviation, but which could not be removed from the data on an a priori basis
2. F-test results significant at the 5% level, indicating that Mg incorporation into the structure is homogeneous.

Discussion and conclusions

While powder XRD data are sufficient to describe the bulk properties and compositional averages of dolomite and magnesian calcite cements, ultrastructural and microchemical data are necessary for a complete description of such phases.

Structurally, these cements are mosaics of submicron sized crystallites which possess a complex heterogeneous microstructure. This microstructure is believed to be due to strain fields associated with high defect densities in the material. Since the heterogeneous microstructure has been observed in dolomites, magnesian calcites, and calcites it is clearly not the result of either Ca/Mg ordering or Mg incorporation.

Electron diffraction patterns of submicron areas of both dolomite and magnesian calcite cements show that a per-

vasive mosaic structure is present. Aside from the mosaic spreading, however, diffraction maxima are discrete points with no apparent diffuseness or streaking. Superstructure diffractions in the dolomite cements are discrete, unimodal maxima, suggesting that there are not variations of Ca/Mg order within individual crystallites. Discrete, unimodal superstructure maxima have also been reported in calcian dolomites by Reeder (1981), Reeder and Nakajima (1982), and others.

STEM microanalytical data indicate that the dolomite cements are more homogeneous in Mg incorporation than the magnesian calcite cements. Furthermore, mean values of $MgCO_3$ incorporation for the dolomite cements cluster about the composition $Ca_{0.58}Mg_{0.42}CO_3$. Land (1967), Gaines (1967, 1977) and others have suggested the possibility of a metastable, calcium rich intermediate of about the composition $Ca_{0.58}Mg_{0.42}CO_3$ in low-temperature dolomite synthesis experiments. In these experiments, the metastable intermediate phase eventually became a stoichiometric, fully-ordered dolomite at sufficiently high temperatures. The non-stoichiometric, partially ordered dolomite cements described here could be similar metastable intermediates.

There appears to be uniform (albeit metastable) solid solution of magnesium in calcite structure up to at least $Ca_{0.69}Mg_{0.31}CO_3$ in these cements. The STEM microanalytical data indicate that there is a markedly greater heterogeneity of Mg incorporation in calcite cements than in dolomite cements.

General comments

Dolomites, non-stoichiometric, partially ordered "protodolomites", and magnesian calcites are presently precipitating in a number of diverse environments. There appear to be many factors involved in the production of dolomite-like order in primary carbonate precipitates. For example, Gaines (1974) suggested that supratidal sabhka dolomites may form due to a decrease in the activity of water. This is certainly not a precondition for the presence of cation order in the fresh water dolomite cements described here. It does appear from the water chemistry data reported by Barnes and O'Neil (1971) for these cements that elevated Mg/Ca ratios in the precipitating solution are necessary. Dolomite formation at low temperatures appears to proceed via a metastable intermediate of about $Ca_{0.58}Mg_{0.42}CO_3$, both in these natural cements and in hydrothermal experiments in which dolomite was produced. Disorder in the carbonate sublattice, described by Gunderson and Wenk (1981), Reeder (1981) and Reeder and Nakajima (1982) has not been observed. This can be inferred from the lack of "*c*" diffractions in electron diffraction patterns, and from the normal intensities of powder XRD diffractions with large carbon and oxygen structure factors (see Schneider, 1976).

While the data described here are highly illuminating with regard to the cation order, ultrastructure and microchemistry of these cements, there are few comparable data available from the large number of environments in which dolomite and magnesian calcite precipitation is occurring. More general interpretations and conclusions are not possible until data are collected from cements precipitating under a wide variety of conditions.

Acknowledgments

We would like to thank the staff of the Electron Microbeam Analysis Laboratory for advice and support during the course of the research. Samples were kindly provided by Dr. Ivan Barnes, USGS, Palo Alto, CA. We thank Dr. Richard Reeder, SUNY Stony Brook, Drs. Ivan Barnes and James O'Neil of the USGS, Palo Alto, Dr. John Valley of the University of Wisconsin, and Drs. Kyger C. Lohmann and B. H. Wilkinson of the University of Michigan for providing comments and criticisms of the manuscript. Support under NSF# EAR81-07529 (DRP) and a Rackham predoctoral fellowship (DFB) is gratefully acknowledged.

References

Allard, L. F., and Blake, D. F. (1982) The practice of modifying an analytical electron microscope to produce clean X-ray spectra. Proceedings of the 17th Conference, Microbeam Analysis Society, 8–20, K. F. J. Heinrich, Ed., San Francisco Press.

Barnes, I. and O'Neil, J. R. (1971) Calcium-magnesium carbonate solid solutions from Holocene conglomerate cements and travertines in the Coast Range of California. Geochimica et Cosmochimica Acta, 35, 699–718.

Blake, D. F. and Peacor, D. R. (1981) Biomineralization in crinoid echinoderms: Characterization of crinoid skeletal elements using TEM and STEM microanalysis. Scanning Electron Microscopy, Inc., III, 321–328.

Blake, D. F., Kocurko, M. J. and Peacor, D. R. (1982) Crystallochemistry of Holocene magnesian calcites from the Gulf Coast of Louisiana. (abstr.) Geological Society of America Abstracts with Program, 14, 445.

Blake, D. F., Isaacs, A. M. and Kushler, R. H. (1983) A statistical method for the analysis of quantitative thin-film X-ray microanalytical data. Journal of Microscopy, 131, 249–255.

Cliff, G. and Lorimer, G. W. (1972) The quantitative analysis of thin metal foils using EMMA-4—the ratio technique. Proc. 5th European Congress on Electron Microscopy. Inst. Physics, London, 140–141.

Gaines, A. M. (1967) An experimental investigation of the kinetics and mechanism of dolomitization. Geological Society of America Special Paper 115, 74–75.

Gaines, A. M. (1974) Protodolomite synthesis at 100 degrees C and atmospheric pressure. Science, 183, 518–519.

Gaines, A. M. (1977) Protodolomite redefined. Journal of Sedimentary Petrology, 47, 543–546.

Goldsmith, J. R. and Heard, H. C. (1961) Subsolidus phase relations in the system $CaCO_3$–$MgCO_3$. Journal of Geology, 69, 45–74.

Goldstein, J. I. (1979) Principles of thin-film microanalysis. In J. J. Hren et al., Eds., Introduction to Analytical Electron Microscopy, p. 88–117, Plenum Press, New York.

Gunderson, S. H. and Wenk, H. R. (1981) Heterogeneous microstructures in oolitic carbonates. American Mineralogist, 66, 789–800.

Kocurko, M. J. (1981) Early cementation by high magnesium cal-

cite from the Gulf Coast of Louisiana. American Association of Petroleum Geologists Bulletin, 64, 734.

Land, L. S. (1967) Diagenesis of skeletal carbonates. Journal of Sedimentary Petrology, 37, 914–930.

Reeder, R. J. (1981) Electron optical investigation of sedimentary dolomites. Contributions to Mineralogy and Petrology, 76, 148–157.

Reeder, R. J. and Nakajima, Y. (1982) The nature of ordering and ordering defects in dolomite. Journal of the Physics and Chemistry of Minerals, 8, 29–35.

Schneider, H. (1976) The progressive crystallization and ordering of low temperature dolomite. Mineralogical Magazine, 40, 579–587.

Manuscript received, January 16, 1984;
accepted for publication, November 19, 1984.